DESIGN OF A HIGH ENTHALPY HYPERSONIC NOZZLE FOR "GHIBLI" PLASMA WIND TUNNEL

D.Guida[1], A.Smoraldi[2] & A.Schettino[3]

[1]CIRA - Centro Italiano Ricerche Aerospaziali, Via Maiorise 81043 Capua (CE)

Abstract

This paper presents a design methodology for high enthalpy hypersonic wind tunnel nozzles, that aims to produce a very uniform airstream at specific Mach number at the nozzle exit section. The methodology is presented after a detailed review of design methodologies for supersonic/hypersonic nozzles. The methodology relies on an iterative optimization procedure based on the Newton-Raphson method, by utilization of a direct design approach in weak coupling with a CFD solver. The direct approach is based on SIVELLS CONTOUR code, without the inviscid boundary layer correction, coupled with the CIRA proprietary Reynolds-Averaged Navier-Stokes solver, NEXT, with the complete thermochemical non-Equilibrium treatments, for gases at high temperature.

In this work it is illustrated how the method is used to design an high Enthalpy axisymmetric nozzle, for the CIRA Hypersonic Reentry wind tunnel GHIBLI, in this case optimized to provide a very uniform flow with specific enthalpy h_0=20 MJ/kg and Mach number M=8, corresponding to a stagnation pressure $p_0=3\cdot10^5$ Pa and to a stagnation temperature T_0=6800K. Numerical simulations of the flow in the optimized nozzle contours showed excellent flow uniformity in the core flow in terms of Mach number variations and a very low flow angularity. The governing equations, numerical technique, objective functions, and design parameters and constrains are discussed along with indication for their choice. Finally, a thermo-structural analysis using commercial code is performed on the nozzle walls, results are analyzed, strengths and limitations of this methodology are discussed and improvement strategies are proposed.

Keywords: wind-tunnel, nozzle, re-entry, optimization

1. Introduction

In hypersonic flight, mechanical stress and extreme heat due to the high enthalpy levels of the flows activated on the surfaces of the aircraft push materials beyond their physical limits.
In last decades, different types of Thermal Protection Systems (TPS) have been developed and introduced, including passive, semi-passive, and active systems.
Increasing demand for Reusable Launch Vehicles (RLVs), but also for sample-return capsules, planetary landers etc., and Reusable spacecraft represents the new goals for human interplanetary missions that are accelerating the search for effective TPS development, even with large investments by private companies [1][2].
So become essential to develop increasingly high-performance TPS, that protect vehicles in these severe conditions, for these reasons the requirements for precision and uncertainty in the design of materials and systems are increasingly stringent. At the present, the source of much of the information cited above is still hypersonic wind tunnels, which consequently require increasingly stringent flow quality requirements. Of the many factors that affect wind tunnel data quality, like measurement techniques, test article integration, data interpretation, flow characterization etc. flow

quality itself, with its very sensitive dependence on the nozzle contour design, still remain a key parameter and the focus of the present paper.

1.1 Design of high uniformity nozzles

The classical approach for designing supersonic tunnel nozzles operating at relatively low enthalpies used the method of characteristics (MOC) corrected with a displacement thickness obtained from boundary layer (BL) calculation to account for the boundary layer formed along the nozzle wall [3]-[5]. Hypersonic nozzles operating at high enthalpy, high Mach number, and relatively low stagnation pressures, such as the GHIBLI wind tunnel case, the development of boundary layers with high thicknesses, which grow along the axial direction of the nozzle, until it reaches a significant percentage of the outlet radius is a deleterious but not avoidable effect. Under such conditions, there is no longer a clear distinction between the central flow and the boundary layer, and appropriate modeling of the viscous interaction between these regions is required. Furthermore, MOC and other analytical solutions, assume the use of a perfect gas model, whereas in this case deviations from this assumption are critical, since the effects of thermochemical non-equilibrium conditions of the gas are present, as along the expansion region [6][7].

To overcome this problem, Korte[8][9] was the first to propose a new design method that coupled a computational fluid dynamic (CFD) solver with a least squares optimization problem to generate a nozzle contour that minimizes the angularity and the change in the Mach number of the outflow. Shope [10] calls this methodology Design-By-Analysis (DBA). The main advantage of the Korte approach is the ability to use CFD solvers that allow the correct modeling of the viscous interaction between the central flow and the boundary layer in high Mach number nozzles. In Korte approach, the flow solution and nozzle contour serve as input to an optimization algorithm that perturbs the contour iteratively, until a uniform nozzle exit flow is achieved.

Korte's approach theoretically allows any combination of CFD solvers and optimization algorithms to be used in the design process, and the accuracy of the design method is limited only by the accuracy of the solver used to perform the flow field calculations and the capacity of the optimizer to reach the desired optimal solution. The present work is based on the same principle but solving a different and fast-convergent optimization problem and using an in-house developed CFD solver capable of taking into account thermochemical non-equilibrium effects. Other authors [11]-[17] have proposed different formulations of Korte's methodology, also this work can be intended as a novel implementation of this approach.

For Instance, the optimization approach utilized by Keeling[11], involves expressing the desired contour as an optimal convex combination of trial configuration. In the work of Matsunaga [13] Shape design optimization has been conducted by employing surrogate-assisted evolutionary algorithms coupled with computational fluid dynamics. In his work the “viscous optimization” has been performed by incorporating viscous simulations without using the more classical boundary layer correction, to evaluate its efficacy in comparison with the former approach. It has been found that the deviation from the design Mach number and the flow deflection from the horizontal direction cannot be minimized simultaneously, and this has been attributed to the constraint associated with the nozzle length. In this work, viscous optimization and thermochemical non-equilibrium effects were optimized via CFD like in the Matsunaga approach, but utilizing a Newton-Raphson iterative approach, aim to minimizing the deviation from the design Mach number and the flow deflection, and maximizing the flow core section by minimizing the length.

2. Optimization Process

For the geometry optimization, a two-step iterative process was performed, based on the Newton-Raphson method which will be illustrated in detail below. The methodology starts by generating different inviscid geometries, calculated using the CONTOUR [5] code developed by Sivells based on the MOC characteristics method, therefore under the hypothesis of a perfect gas with an assigned and constant ratio between the specific calories. The nozzles thus obtained were solved using the an in house developed CFD code, verifying whether or not the desired conditions were obtained in the test section for the imposed stagnation conditions, effectively creating a weak coupling between the CFD solver that exploits analytical field solutions and a direct design geometries generator. The

solutions thus obtained were used to carry out a new estimation of the equivalent input value for γ, in the CONTOUR code for the geometry generation and intermediate section (cutting length), which become the control variables of the optimization problem. According to a discrete multivariant Newthon-Raphson algorithm, iterating the steps described, until obtaining the desired conditions in terms of Mach uniformity and angularity in a predetermined “core flow” region, which become the objective functions of the iterative algorithm. More details are given below.
The method permit the design of nozzle for specified stagnation condition, and it is used to design an asymmetric nozzle, for the CIRA Hypersonic Re-entry wind tunnel GHIBLI, in this case optimized to provide a flow with specific enthalpy h_0=20 MJ/kg and Mach number M=8, corresponding to a stagnation pressure p_0=3·105 Pa and at a stagnation temperature T_0=6800K. In order to achieve the convergence of the problem, all the different nozzles inviscid profile have been numerically simulated with the same, input conditions, chemical model, transport model, and fixed temperature of the nozzle internal wall ($T_{wall_int=}$300 K) with the hypothesis of full catalytic wall, and with different gamma values as selected by the discretized Newton Raphson method.

2.1 Setting of initial conditions

Theoretically, an endless set of geometry might result in leading in a parallel and consistent flow within a specific region of the exit section. However, it's evident that certain design decisions may outperform others. Numerous elements can influence the flow's quality, yet selecting optimal initial design strategies can notably enhance certain effects.
For the calculation of the inviscid profiles, as mentioned, a Fortran based code named, developed by Sivells was used (in this case without using the classic boundary layer thickness correction based on the resolution of the momentum equation by numerical integration or by semi-empirical correlations). This code allows many different choices in profile generation.
The geometry profile selected to generate the different nozzle in this work is axisymmetric, and the continuous curvature is obtained through the specification of a central distribution of the Mach number, such that the first and second derivatives are compatible with a nearby transonic solution
the throat and with radial flow near the inflection point, and such as approaching zero at the design Mach number. From sonic point where radial flow is assumed to begin, the velocity distribution is described by a three or fourth-degree polynomial, after a radial flow is assumed. Downstream where uniform flow begins, the Mach number distribution is described by a four or fifth-degree polynomial. The transonic solution is used merely to relate the throat radius ratio R (the ration between the throat radius r* and the throat curvature radius Rr* Figure 1) with the displacement e of the sonic point on the axis from the geometric throat, and with the derivatives of the axial velocity distribution at the sonic point. The coefficients of the polynomials are chosen such that the second derivative of the axial velocity is continuous throughout and is zero at the exit section.

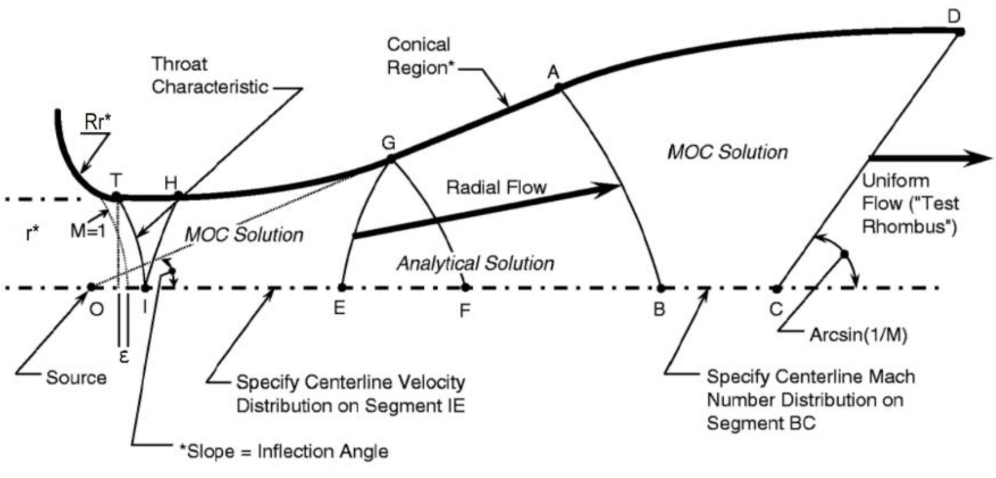

Figure 1 – Inviscid contour design by Sivells CONTOUR, adaptation form Shope [13]

The CONTOUR code allows other types of choices, such as the possibility of creating planar nozzles (not preferable as they produce fewer uniform flows and are more subject to dimensional stability problems), or use different types of polynomial distributions, also to calculate the entire nozzle profile starting from the transonic solution. For the choices made in this work, what can be defined as a cubic-radial-quadratic profile is obtained (respectively in sections IE-EB-BC, Figure 1), with transonic solution in the throat.

The curves thus obtained were interpolated using a spline function and smoothed. For the converging section, a cubic polynomial geometry was used, for the sole purpose of mechanically and adequately interfacing the nozzle throat with the electric arc heater. In this implementation, the fluid stagnation conditions do not have a direct effect on the profile design, as the throat section is fixed, but they essentially influence the thickness of the boundary layer which in this case was not used.

To generate the different geometries, these choices were kept the same for all the profiles, the only parameters varied were, specific heat ratio, the exit radius in order to keep the throat radius Rr fixed (the Sivells code allows the control directed on the exit radius but not on the throat radius r*), and appropriately the Mach distribution along the axial profile to avoid solution divergence problems. The axisymmetric profiles, generated in this way, differ from each other in the final length of the nozzle and in the exit radius (Figure 2).

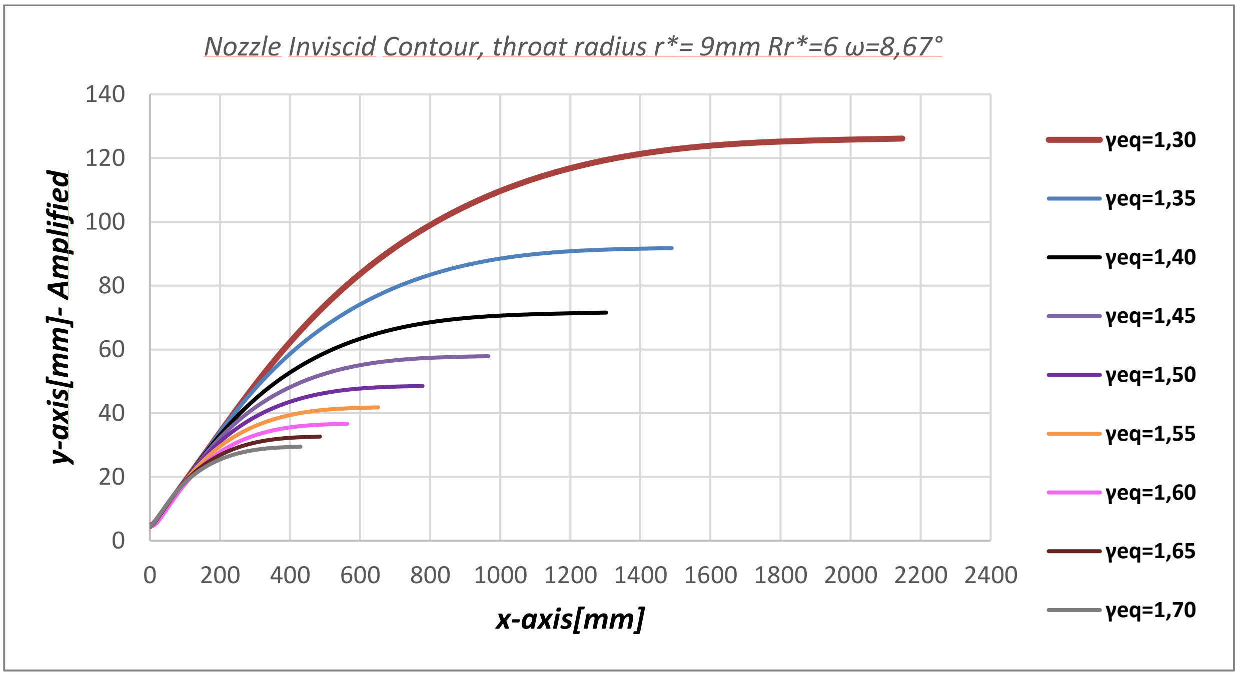

Figure 2 – Nozzle Inviscid Contour, for γ variation

In general, for hypersonic tunnels flows with greater uniformity, which is a primary criterion for tunnel tests, especially for aerodynamic tests, this uniformity only can be achieved with very long nozzles, therefore with small bending angles (Shope [10][13] recommends keeping above 12° degrees, in the present case an angle of 8.67° degrees was chosen.) On the other hand, for high enthalpy systems, nozzles that are too long produce large losses of the often expensively obtained total enthalpy. For an electric arc system like Ghibli, very short nozzles are usually chosen with the awareness that a very important part of the flow quality will be sacrificed. However, nozzles that are too short often have large deflection angles (for instance 15°), which increases the possibility of disastrous flow separation. Furthermore, short nozzles tend to have a small radius of curvature of the wall at the throat, comparable to the radius of the throat itself, which not only makes accurate machining more difficult, but also increases sensitivity to production defects, assembly and above all worn effects, the throat area being the most thermo-structurally stressed, as will also be shown later. In the present work, in order to reduce this sensitivity, a ratio between curvature radius and throat radius equal to 6 was chosen. Finally, short nozzles with large flow expansion rates tend to be highly affected by the effects of non-equilibrium, while long nozzles give the flow more transit time to relax towards equilibrium.

2.2 First step of optimization

The objective function has been defined so that the optimization algorithm tries to find the nozzle shape that produces flow with minimal deviation from the design Mach number at the nozzle exit plane, verifying that the flow deflection from the horizontal directions is approximatively 0 and that the other desired characteristics are obtained. Note that this design method is not limited to just achieving an optimal Mach number and flow angle; the nozzle contour can also be optimized for other flow parameters (e.g. static pressure, temperature, enthalpy and velocity). In the case of the GHIBLI nozzle, no semi-empirical Edenfield type correlations [4] are available in the literature for the boundary layer thickness operating in the hypersonic regime at similar enthalpy levels, where no net separation exist between the core flow and the boundary layer.

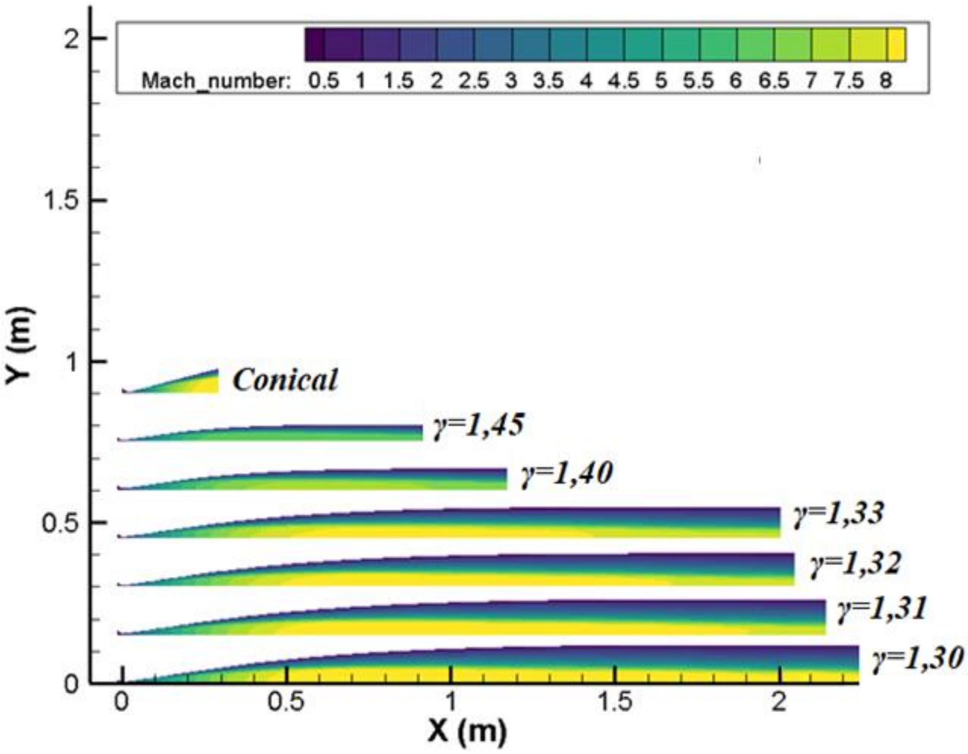

Figure 3 – Nozzle Inviscid Contour Solutions, for different equivalent γ, Twall=300 K, P_0=3bar, H_0=20MJ

The viscous iteration problem and the non-equilibrium problem of the working fluid were both circumvented by introducing the concept of "equivalent γ", γ_{eq}, to be used to generate new geometries, solution adopted also in other real gas enthalpy nozzle design **Errore. L'origine riferimento non è stata trovata.** what in a real gas problem would represent the ratio of specific heats, in this case it becomes only a control parameter for the generation of different geometries, but also the gas constant could have been chosen. The iterative optimization process illustrated in Figure 4 was followed for profile optimization, and represent the first of a twostep process. Once the non-viscous profile (MOC) has been calculated in the hypothesis of a perfect gas with a ratio between the specific heats, γ, assigned and constant, and initially equal to 1.4, without however implementing the boundary layer correction solutions (BLC), but variable following a Newton Raphson algorithm, in order to obtain new contours, the profiles thus obtained were used to find field solutions through a series of numerical simulations obtained using the NEXT codes (complete solution of two-dimensional Navier-Stokes equations in thermal and chemical non-equilibrium), thus verifying that the desired conditions have been achieved or not in the selection process. The information at each iteration was then used to make a new estimation of the equivalent γ as in through the Newton-Raphson method, although other methods are possible.

$$\gamma_{n+1} = \gamma_n - \frac{M(\gamma_n)}{M'(\gamma_n)} \quad (1)$$

Convergence is achieved by iterating the steps described until the design Mach number is obtained in the output section. For the profiles thus obtained, the evolution of the flow field was analysed, along the entire nozzle, obtained by imposing a stagnation pressure of 3 bar of and an enthalpy of 20MJ/Kg corresponding to a stagnation temperature of 6800K, simulating for comparison also the current nozzle (Conical 15°).

In this way the CIRA NExT numerical solver [18] 3D RANS solver implicitly took into account the effects of thermochemical non-equilibrium and viscous interaction of the gas at very high temperatures, overcoming the implicit limit of the Sivells code and the characteristic method, to function only with the very deleterious hypothesis of an ideal gas.

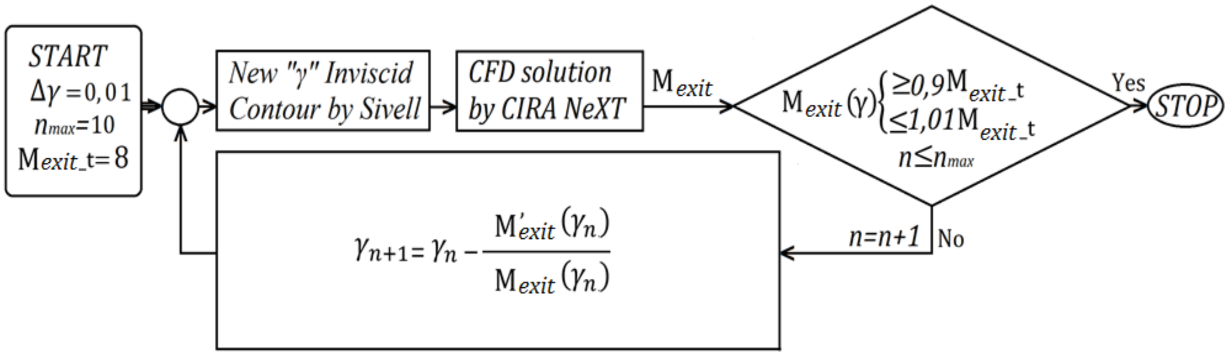

Figure 4 – Optimization Procedure Newton-Raphson based algorithm- Step1/2

Convergence was however achieved, on γ=1.33 after 5 iterations, using the one calculated in the cell shown in the figure as the target Mach number which becomes the objective function. In this way the first step of the optimization process was closed and the profiles generated, under a series of simplifying hypotheses, guarantee zero angularity of the outgoing flow.

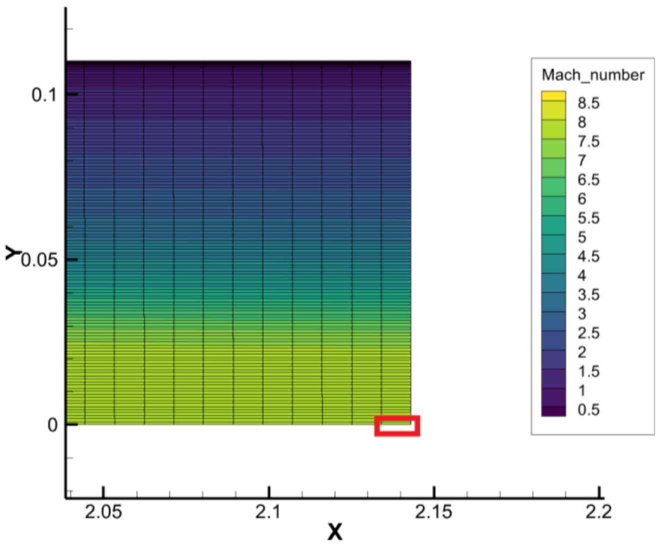

Figure 5 – Contour of Mach at exit section, target Cell for design Mach number Highlighted in red

The uniformity and angularity of the flow thus obtained at the exit section were then verified. Under such conditions of low pressure and high enthalpy, there is a massive growth of the boundary layer thickness, and a strong viscous interaction effect. In these conditions the core flow zone and the limit state zone largely merge, making the use of the boundary layer concept inappropriate. This effect is highly deleterious for a wind tunnel, as flow uniformity is guaranteed only in a very limited core flow section which represents only a minority percentage of the exit section, and therefore of useful testing zone.

2.3 Second step of optimization

With the dual objective of obtaining a shorter nozzle and a lower evolution of the boundary layer, it was therefore decided to cut the nozzle at a certain intermediate section defined as:

$$X = x[mm]/Lmax[mm] \tag{2}$$

Such an important growth of the boundary layer, leads to a change of the fluid dynamic quantities along the axial profile, which will follow its evolution. To then distinguish the limit state and core flow regions, the concept of uniform core flow was introduced, and defined as follows:

$$\delta_u(\gamma, X) = \{y | 0{,}99 M(0,\gamma,X) < M(0,\gamma,X) < 1{,}01 M(0,\gamma,X),\ 0 < y < Y(x)max[mm]\} \tag{3}$$

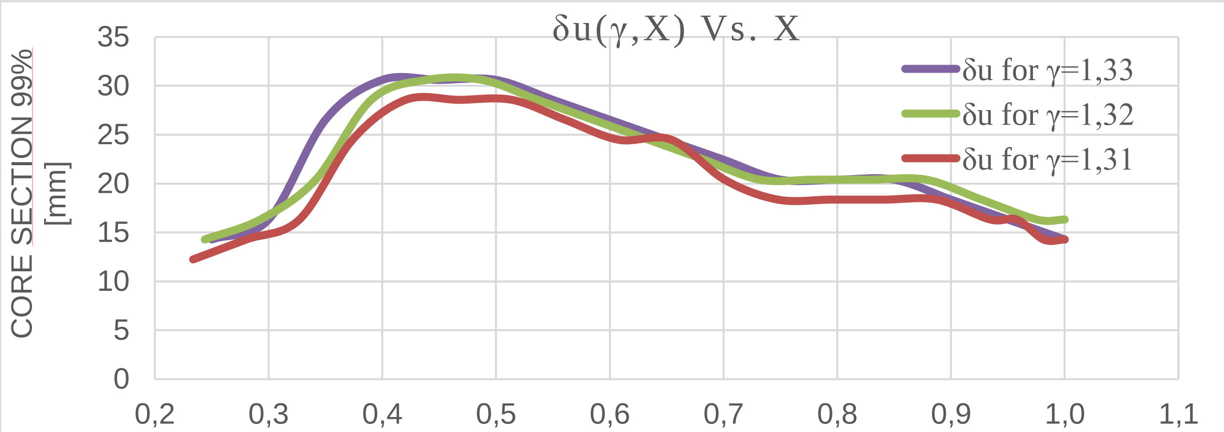

Figure 6 – Evolution of uniform Mach core flow, along the axial direction for three geometries

That is, the core flow region is considered uniform such that the Mach lines varies by less than +/- 1% along the radial direction, compared to the value calculated in the centerline cell.

It is a very stringent condition that aims to obtain a very high uniformity of the test flow, but obviously it is possible to take larger core zones into consideration, degrading the uniformity requirements. The width of the uniform mach zones shows congruence for the different geometries. For all the simulated geometries the trend of the core flow zone is first increasing and then decreasing interspersed with two almost uniform touches.

In Figure 6 the core section was plotted along the nozzle axial symmetry axis; this velocity distribution differs greatly from the velocity profile that had been imposed in the SIVELLS code for nozzle generation.

A trend of the average Mach number along the axis of axial symmetry was obtained defined in eq.4:

$$M_{\delta u}(\gamma, X) = \frac{1}{\delta_u} \int_0^{\delta_u} M(\gamma, X, y)\, dy \tag{4}$$

As shown, this trend maintains good consistency for all geometries; for example, 3 cases close to the solution are illustrated in the figure.

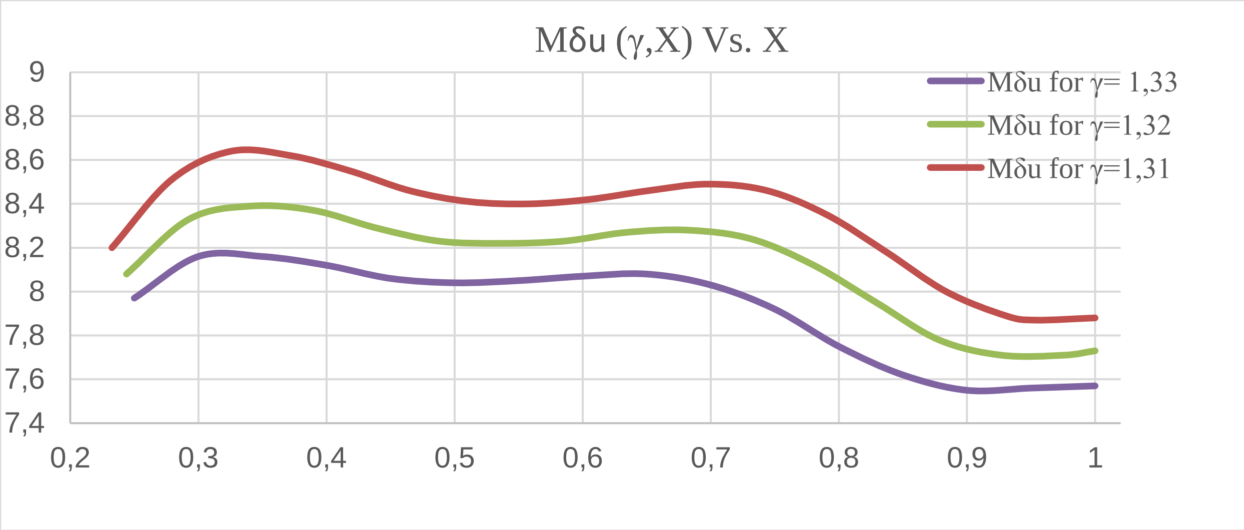

Figure 7 – Evolution of uniform core flow, Mach profiles $M_{\delta u}$ along the axil direction for three geometries

The evolution of the Mach profiles along the axial direction is obviously correlated to that of the limit state, or more precisely of strong viscous interaction.

Finally, the maximum angularity of the flow along the axial profile in the core flow region was verified:

$$\vartheta_{\delta_u}(\gamma, X) = \max|\vartheta_{\delta u}(\gamma, X, y)|_{0<y<\delta_u} \tag{5}$$

Also, in this case, the three geometries generated flow fields, show a congruent and similar characteristic, where, as was logical to expect, it is observed that globally the flow angularity asymptotically tends towards zero. However, around 65% of their length, in the nozzles the strong evolution of the viscous region tends to greatly affects the core flow, in fact the angularity increase in the intermediate section. This effect is undoubtedly deleterious and suggests cutting the nozzle around 40%-50% of the its length, or even before but scarifying part of its angularity.

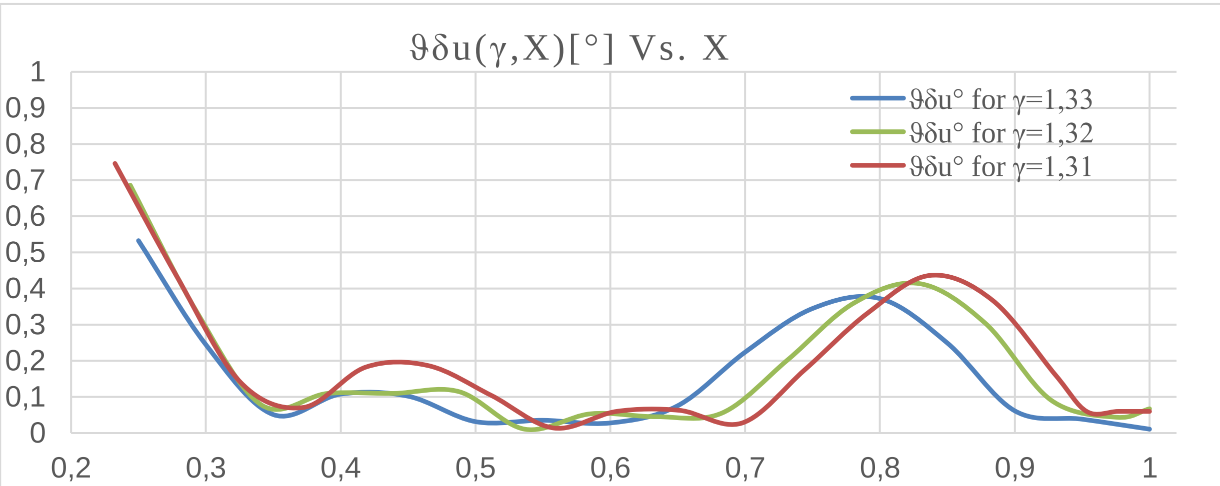

Figure 8 – Evolution of max flow angularity in the core flow, Mach profiles $\vartheta\delta u$ along the axial direction for three geometries

In the case in question this will lead to having nozzles of approximately one meter in length, this choice will help the integration of the same into the existing facility, reduced production costs and to contain the total enthalpy loss. These constraints also allow us to obtain a larger region of uniform Mach, which is greatly reduced along the axial section due to the strong growth of the boundary layer. In operational terms this translates into the possibility of being able to test larger items at the same energy costs.

To this end, starting from the equivalent gamma of 1.31 found in the previous iterative optimization process, a second optimization step was launched, which is always based on a discrete Newton Raphson method but in this case multimodal, where the Control variables became the range and intermediate nozzle length.

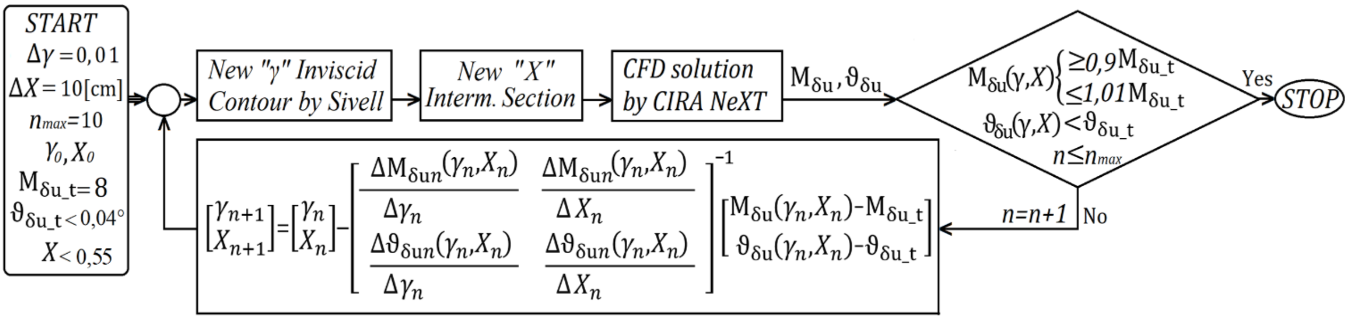

Figure 9 – Optimization Procedure Newton-Raphson based algorithm step 2/2

The algorithm iterates through the various geometries and sections looking for the specific couple that achieves the input requirements, i.e. the desired Mach number $0.99Mt < M_{\delta u} < 1.01Mt$ and angularity $\vartheta_{\delta_u} < 0.1$ in the core flow region. A further condition imposed was to choose a length less than 0.55% in order to maximize the uniform Mach region and imitate the thick boundary layer grow. This present double optimization Newton-Raphson based iterative algorithm is not reliably convergent effectively, but a manually controlled direct search is performed, and this approach was found successful and satisfactory converging on $\gamma = 1.31$ and X=0.50 %. The same methodologies can be applied to generate nozzle for different conditions.

2.4 Result for GHIBLI high enthalpy Mach=8 case

The design procedure is demonstrated by design of nozzle for a Mach number 8 and H0=20MJ/Kg for Ghibli arc-heated test facility. For comparison, the results obtained for 3 types of Nozzle are shown, the conical one currently operational, the contoured one obtained at the first optimization step with the objective of obtaining the output Mach target and the final optimized one which is still of the contoured type but shortened. The figure shows the profiles of the Mach number, its first derivative and the angularity of the flow obtained in the exit section for the 3 different geometries. As you can see, the conical nozzle does not reach the target output Mach number which is 9.25. In the exit section, along the radial profile the Mach number varies almost linearly starting from zero at the center until reaching an angularity of 15°, i.e., equal to that of the wall and then immediately going to zero in the boundary layer. Even the Mach number does not remain uniform in the core flow region, as can also be seen from its derivative. Although this type of nozzle has the advantage of being very short, it cannot guarantee a highly uniform flow, which is desirable for a tunnel.

The nozzle optimized in the first step, however, presents a maximum angularity of 0.43° along the entire radial profile in the exit section, the cut nozzle, as expected, presents a slightly greater maximum angularity at parts of 1.25°.

If instead we focus our attention on the useful core flow area, as previously defined, we first notice that the useful area with high uniformity is equal to 372.4mm^2 corresponding to a radius δ_{un} of 12 mm, 780.8mm2 corresponding to a radius of 16mm 2740mm^2 corresponding to a radius of 30mm.

The maximum angularity of the Mach in these regions is instead 1.50° for the conical, 0.07° for the contoured full length and < 0.04° for the contoured cut. In fact, the cut globally improves the uniformity and angularity characteristics of the field in the useful area.

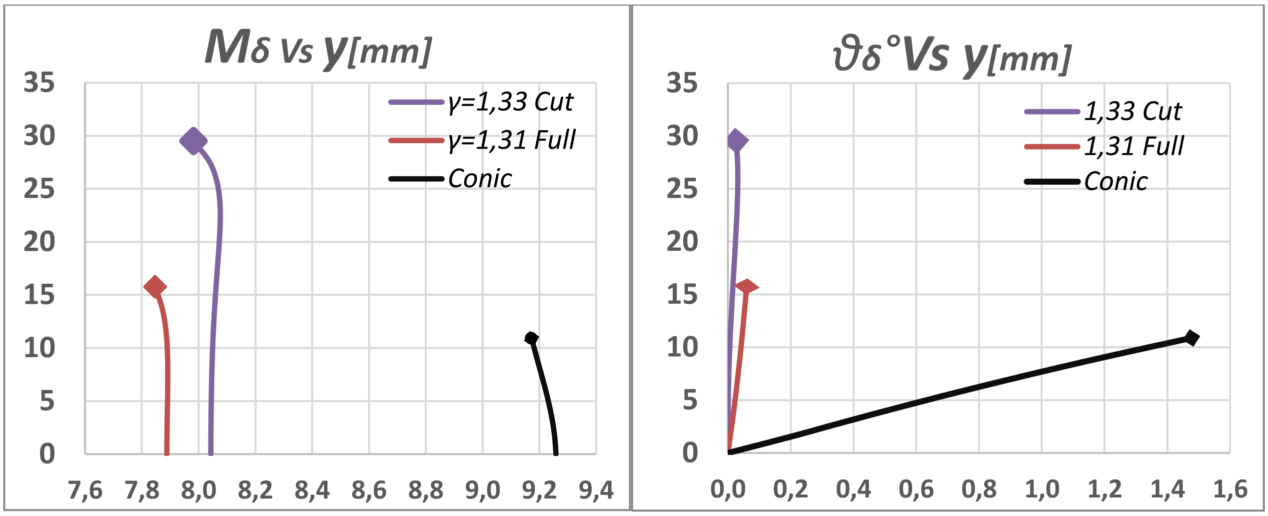

Figure 10 – High Uniformity Flow area section for the different nozzle

2.5 CFD Details

Numerical CFD simulations performed to achive the design conditions, have been carried out with the in-house CIRA code, NEXT[18], that solves on a multi-block structured grid, the Reynolds Averaged Navier–Stokes (RANS) equations in a density based finite volume approach, with a cell centred, Flux Difference Splitting at second order, ENO-like, upwind scheme for the convective terms. In the CAST code solver is implemented the Park '89 chemical model with air - 5 species [N2, O2, NO, N, O], involved in 17 reactions [20], implemented to account for coupling between dissociation and vibration. The rotational temperature of molecules, Tr is assumed in thermodynamic equilibrium with the translational one, T. Vibrational and roto-translational modes exchange modelled by the classical Landau–Teller non-equilibrium equation, with average relaxation times taken from the Millikan– White theory [21], modified by Park [19]. The transport models employed in these simulations treat the viscosity of the single specie evaluated by a fit of collision integrals calculated by Yun and Mason [22], the thermal conductivity is calculated by means of the Eucken's law, the viscosity and thermal conductivity of the gas mixture are then calculated by using the semi-empirical Wilke formulas [23]. Finally, the diffusion of the multicomponent gas is computed through a sum rule of the binary diffusivity of each couple of species (from the tabulated collision integrals of Yun and Mason [22]).

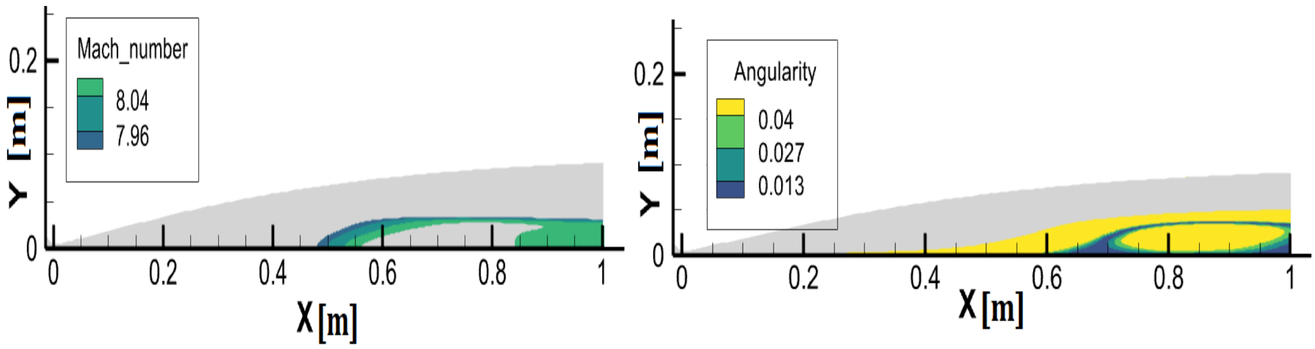

Figure 11 – High uniformity Mach and low angularity Contours Obtained

3. Thermo-structural Analysis of Nozzle Contour near Throat Region

The design of the cooling circuit to be adopted and the prediction of the thermal and mechanical stresses to which the nozzle is subjected during its operation will be illustrated below using ANSYS simulations coupled with CFD accounts. In this case the nozzle analysis was not performed for all the length, but only for the most thermally stressed section, near the non-equilibrium zone throat and in the first expansion region, where the temperatures are still very close to the stagnation temperature.

The CFD accounts were carried out under the hypothesis of an adiabatic wall, fully catalytic and at a fixed temperature of 300K. A weak coupling was then created with a FEM code, Ansys specifically, to estimate the real wall temperature. The wall heat flow, as calculated by the CFD accounts, was used as a heat source on the internal surface of the nozzle for the heat account on Ansys, which by imposing a condition of convective heat exchange on the external surface h_{cw_ext} =52418 [W/m^{2}K]. of the same, neglecting the contribution radiative and considering the other nozzle surfaces adiabatic. The FEM code provides a new internal wall temperature, used for a new estimation of the heat flow, in an iterative process by repeating these last two steps until the calculation wall temperature convergence is achieved:

$$|T_{w\_n} - T_{w_{n-1}}| = \Delta T < 1K \quad (6)$$

From the iterative procedure just described, a new temperature distribution was obtained on the Nozzle profile. Convergence on the wall temperature was achieved after two iterations. The accounts converged quickly as the heat exchange was convective on the internal wall, dominated by the stagnation temperature of the fluid and equal to approximately h_{cw_int} =56666 [W/m^{2}K].

$$q_n = h_{C\_int\_w\_n}\left(T_0 - T_{w\_n}\right) \quad (7)$$

$$h_{c_{w_{int_{n+1}}}} = \frac{q_n}{\left(T_0 - T_{w_{int_{n+1}}}\right)} \quad (8)$$

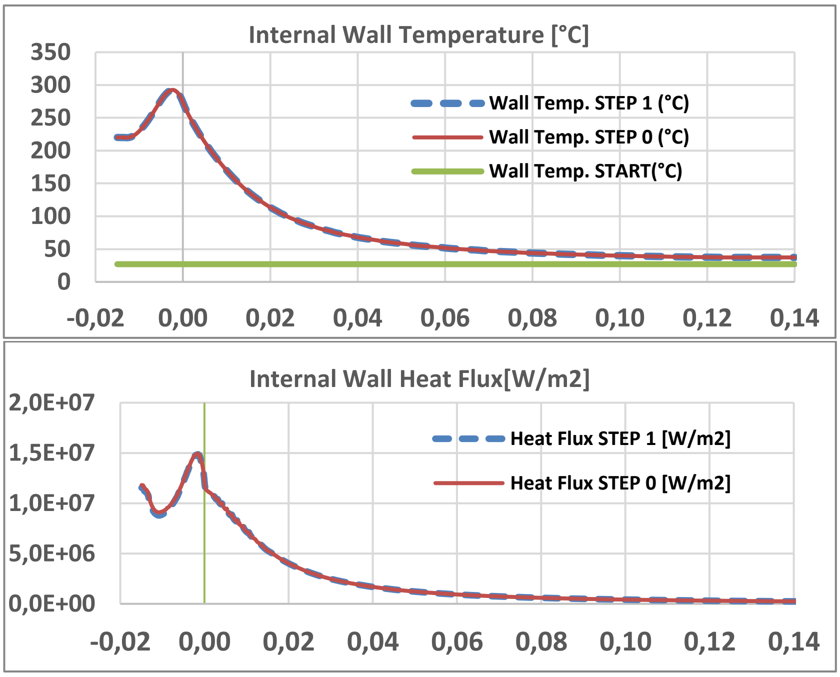

Figure 12 – Internal Wall Heat flux and Temperature

Once the wall temperatures were estimated, we moved on to the thermo-structural analysis and then to the design of the cooling circuit. The thermal analysis highlights that, thin walls, specifically for3 mm thick, to be made of high purity copper with a thermal conductibility of 394 [W/mK] guarantee, despite such harsh conditions, adequate cooling of the internal wall, which in the greater thermal stress, i.e. near the throat, never exceeds 600K despite an estimated heat flow of 14MW/m^2.

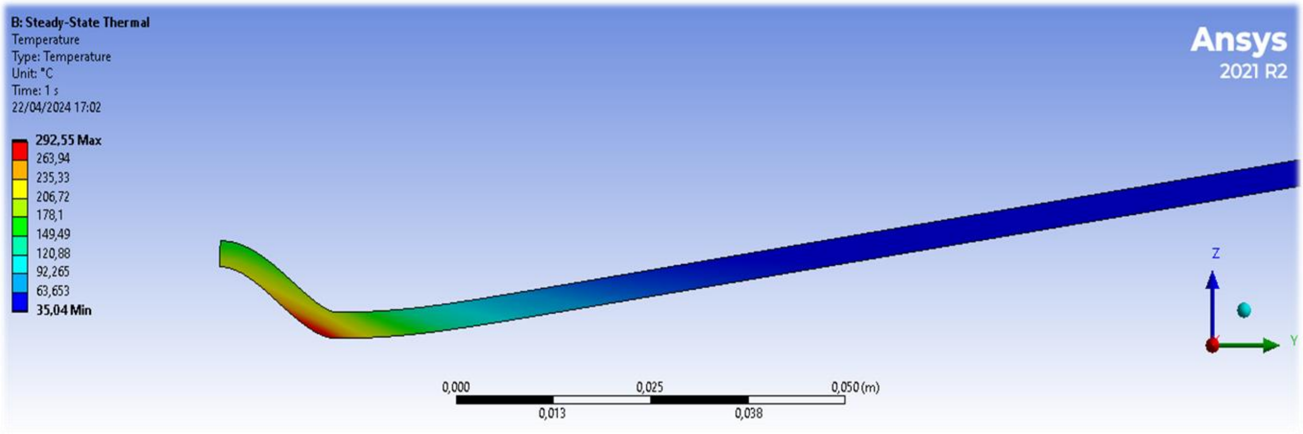

Figure 13 – Steady State Temperature Distribution

As regards dimensional stability, as a first approximation we can hypothesize that for the type of installation to be carried out, this will be mechanically constrained at its ends, while on the outside it will be cooled by water at a maximum pressure of 20 bar (nominal limit of the circuit cooling). In these conditions, starting from the temperature field thus calculated, the stresses (3.6e-5mm/mm maximum von Mises equivalent elastic deformation) and the deformations (0.05mm maximum and 0.03mm in the section of throat) to which the nozzle is subjected during its operation in nominal conditions. The results obtained highlight that the dimensional stability of the nozzle operating in this way is guaranteed.

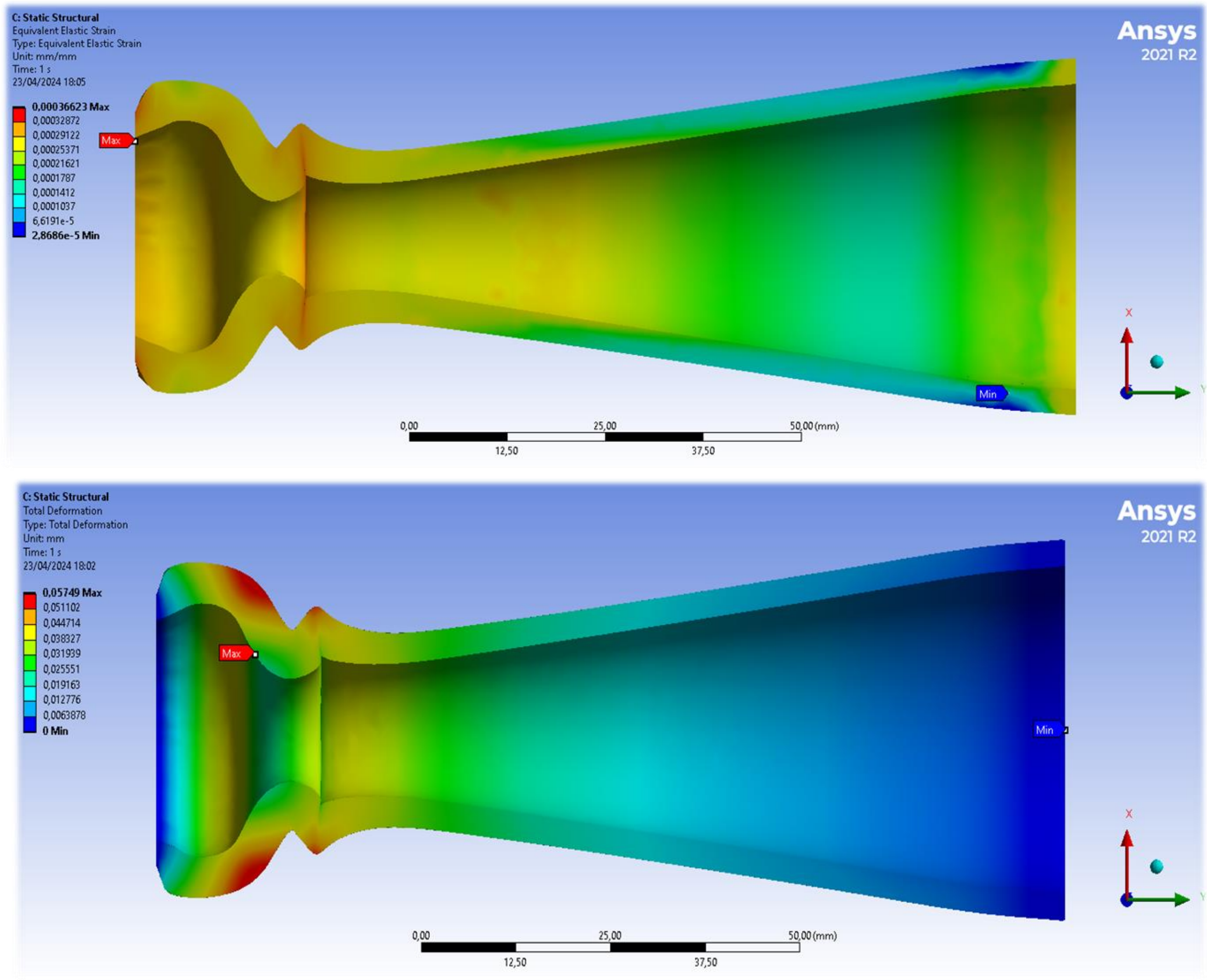

Figure 14 – Equivalent Elastic Strain and Total Deformation

3.1 Cooling circuit design

For the cooling circuit, demineralised water will be used as the working fluid, making use of the circuits already served by the system.
The cooling circuit will consist of a jacket, in order to guarantee homogeneous cooling of the nozzle walls. As anticipated, the entire circuit was designed to guarantee an operating temperature of the internal surface of the throat below 600K, for a flow with an enthalpy of 20MJ/kg this translates into an estimated convective heat transfer coefficient in the throat, from which Nu=268 was obtained.

$$h_{cw\_ext} = kw{*}Nu/D_{eq} = 52418\ W/m^2 \qquad (10)$$

To estimate the Reynold number, in this condition of forced convective heat exchange in internal channels, inverse use was made of the Gnielinski [23] correlation:

$$N_u = \frac{(f/8)(Re-1000)Pr}{1+12{,}7(f/8)^{1/2}(Pr^{2/3}-1)} \qquad (11)$$

Although the Dittus-Boelter and Sieder-Tate equation are easily applied, errors as large as 25% may result from their use (58% for the conditions in examination). Such errors has been reduced by using the more recent but generally more complex correlations of Gnielinski. This equation validates tubes over a large Reynolds number range, including the transition region. For the purposes of this article, where we intend to be conservative, it is preferable to use the value estimated by Gnilelinski correlation which appears to be the lowest.
In this case it is therefore necessary to create a Nusselt number of 180, by imposing the Reynolds $Re=\rho v D_{eq}/\mu=71982$. So it was necessary to create a maximum speed of the water in the throat of approximately 29m/s, where the annular channel reaches the minimum section of $51mm^2$. In the conditions implemented, this speed results in a flow rate of 1.5kg/second of water, which is approximately half the availability of the system in terms of flow rate. It would therefore be possible to use the nozzle also for higher enthalpies with the same thermal stress.

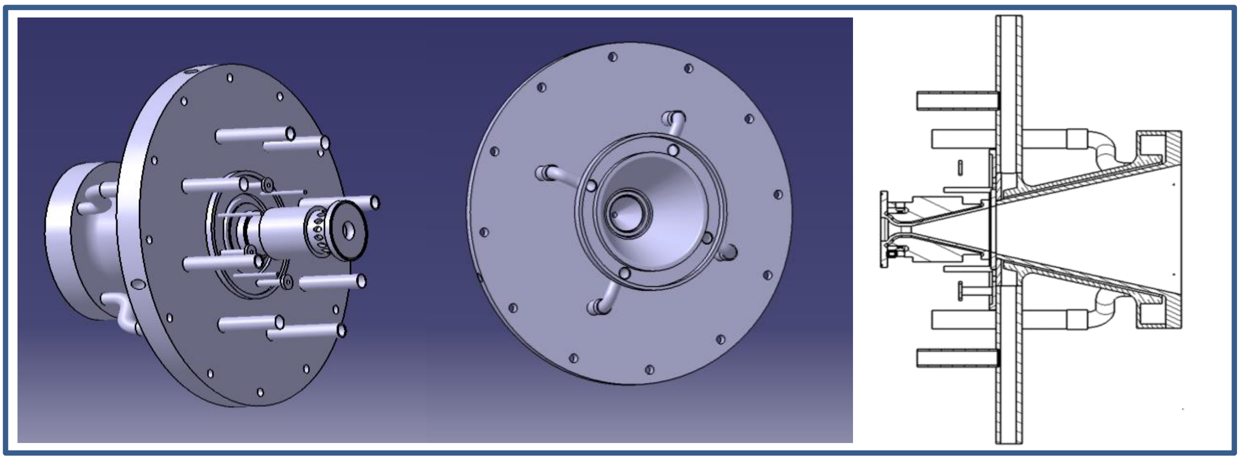

Figure 15 – Sketch Views and Side View of Nozzle throat region cooling circuit

Finally, the maximum expected pressure drops were estimated, using the Darcy-Weisbach relationship, and estimating the Darcy friction factor, using the Coolebrook correlation

$$\frac{1}{\sqrt{f}} = -2log\left(\frac{\varepsilon}{3{,}7Deq} + \frac{2{,}51}{R\sqrt{f}}\right) \qquad (12)$$

The Darcy friction factor f=0.022 was estimated using the typical roughness of smooth copper tubes ε[mm]= 0.0015. The pressure drop thus estimated is less than 4 bar, well within the current availability of the system's cooling circuit, the maximum limit of which is 20 bar.

4. Conclusions ad final remarks

In this work, a design methodology for high-enthalpy hypersonic wind tunnel nozzles was presented, which aims to produce a very uniform airflow at a specific Mach number in the exit section of the nozzle. It is clear that for the operating conditions to be achieved, with a high enthalpy flow in thermochemical non-equilibrium, it is not possible to apply the MOC. The methodology presented is based on an iterative optimization procedure based on the Newton-Raphson method, using a direct design approach in weak coupling with a CFD solver. In this work this methodology was shown in detail and then applied to the design of a high enthalpy axisymmetric nozzle, for the CIRA wind tunnel GHIBLI[25] for h_0=20 MJ/kg and Mach M=8, showing excellent flow uniformity in terms of Mach number changes and a very low flow angularity. This methodology supports, theoretically, the coupling of any curve generator with any solver (although convergence is not always guaranteed).
For lower stagnation pressures, it would be possible to use a Direct Monte Carlo Simulation[26] instead of the CFD code to better take into account the re-rarefaction effects.
A final observation is made on the real effects that influence the quality of the flow. First, the nozzle should not be expected to “clean up” an incoming stream which is highly non-uniform, as can be the one produced in arc-jet type plants. +Further details were given on the thermo structural analysis of the same, and on the related cooling circuit.

Copyright Statement

References

[1] D. Ellerby, et al., Overview of Heatshield for Extreme Entry Environment Technology (HEEET), 15th International Planetary Probe Workshop, Boulder, CO, June 2018.

[2] Obinna Uyanna and Hamidreza Najafi, Thermal protection systems for space vehicles: A review on technology development, current challenges and future prospects Acta Astronautic Volume 176, November 2020, Pages 341-356 https://doi.org/10.1016/j.actaastro.2020.06.047

[3] Sivells J, Aerodynamic Design of Axisymmetric Hypersonic Wind-Tunnel Nozzles, Journal of Spacecraft and Rockets, Vol. 11, No. 11, 1970, pp. 1292–1299. doi: 10.2514/3.30160.

[4] Edenfield, E.E., Contoured Nozzle Design and Evaluation for Hotshot Wind Tunnels, AEDC TR-72- 48 - Washington, 1972

[5] Sivells, J.C, A Computer Program for the Aerodynamic Design of Axisymmetric and Planar Nozzles for Supersonic and Hypersonic Wind Tunnels, AEDC TR-78-63 - Washington, 197

[6] Hall, J.C., Treanor, C.E, Nonequilibrium Effects in Supersonic Nozzle Flows, AGARD AG-124, London 1967

[7] Junmou Shen *,Zongjie Shao,Feng Ji *,Xing Chen,Hongbo Lu and Handong Ma, High Enthalpy Non-Equilibrium Expansion Effects in Turbulent Flow of the Conical Nozzle, *Aerospace* 2023, *10*(5), 455; https://doi.org/10.3390/aerospace10050455

[8] Korte J, Kumar A, Singh D and Grossman G, Least-Squares/Parabolized Navier-Stokes Procedure for Optimising Hypersonic Wind-Tunnel Nozzles, Journal of Propulsion and Power, vol.8, num.5, 1992

[9] Korte J, A CFD-based Aerodynamic Design Procedure for Hypersonic Wind-Tunnel Nozzles, 70th AGARD Fluid Dynamics Panel Symposium, Theoretical and Experimental Methods in Hypersonic Flows, Torino, 1992

[10] Shope F, Contour Design Techniques for Super/Hypersonic Wind Tunnel Nozzles, 24th Applied

Aerodynamics Conference, 5 - 8 June 2006, San Francisco, California

[11] Keeling, S.L. A Strategy for the Optimum Design of Nozzle Contours, AIAA 93-2720, 28th AIAA Thermophysics Conference - Orlando, 1993

[12] Frederick L. Shope, Design Optimization of Hypersonic Test Facility Nozzle Contours Using Splined Corrections, AEDC-TR-04-2, March 2005

[13] Matsunaga M, Fujio C, Ogawa H,∗, Yoshitaka Higa Y, Handa T Nozzle design optimization for supersonic wind tunnel by using surrogate-assisted evolutionary algorithms, Aerospace Science and Technology Volume 130, November 2022, 107879 https://doi.org/10.1016/j.ast.2022.107879

[14] Wang Y, Theories and methods for designing hypersonic high-enthalpy flow nozzles, Chinese Journal of Aeronautics March 2021 DOI:10.1016/j.cja.2021.01.018

[15] Fernandes, T., Souza, A. and Afonso, F. A shape design optimization methodology based on the method of characteristics for rocket nozzles. CEAS Space J 15, 867–879 (2023). https://doi.org/10.1007/s12567-023-00511-1

[16] Shenghao Wu, Daxiong Liao, Jiming Chen, Qin Chen, Haitao Pei Supersonic Nozzle Optimization Design with Spline Curves Fitting the Nozzle Profiles Journal of Northwestern Polytechnical University, Volume 36, Issue 4: 785 - 791 (2018), https://doi.org/10.1051/jnwpu/20183640785

[17] Chan W, Jacobs P, Smart M, Grieve S, Craddock C, Doherty L, Aerodynamic Design of Nozzles with Uniform Outflow for Hypervelocity Ground-Test Facilities Journal of Propulsion and PowerVolume 34, Number 6November 2018 https://doi.org/10.2514/1.B36938

[18] F.Scortecci et Al, Disegno dell'ugello per una galleria ipersonica ad alta entalpia, XIV Congresso Nazionale AIDAA, Napoli, Italy. 1999

[19] Giuliano Ranuzzi and Luigi Cutrone NUMERICAL SIMULATION OF LRE AND HRE REACTING FLOWFIELDS67th International Astronautical Congress 2016, Paper ID: 34544

[20] Flament, C. “Chemical and Vibrational Nonequilibrium Nozzle Flow Calculation by an Implicit Upwind Method”, 8th GAMM Conference on Numerical Methods in Fluid Mechanics, Delft, 1989

[21] C. Park, Two-temperature interpretation of dissociation rate data for n2 and o2, in: Aerospace Sciences Meetings, American Institute of Aeronautics and Astronautics, 1988, https://doi.org/10.2514/6.1988-458.

[22] R.C. Millikan, D.R. White, Systematics of vibrational relaxation, J. Chem. Phys. 39 (12) (1963) 3209–3213.

[23] K. Yun, E. Mason, Collision integrals for the transport properties of dissociating air at high temperatures, Phys. Fluids 5 (4) (1962) 380–386. [19] R.N. Gupta, J.M. Yos, R.A. Thompson, K.-P. Lee, A review of reaction rates and thermodynamic and transport properties for an 11-species air model for chemical and thermal nonequilibrium calculations, to 30000 k

[24] John H. Lienhard IV and John H. Lienhard, V A Heat Transfer Textbook, Phlogiston Press, 2012

[25] Purpura at al., The GHIBLI plasma wind tunnel: Description of the new CIRA-PWT facility Acta, Volume 61, Issues 1–6, Pages 331-340, June–August 2007, https://doi.org/10.1016/j.actaastro.2007.01.046

[26] Davide Cinquegrana, Raffaele Votta and Eduardo Trifoni Rarefaction Effects in NASA arc jet testing at SCIROCCO facility, AIAA 2017-4450, Published Online:2 Jun 2017, https://doi.org/10.2514/6.2017-4450